



NRL/FR/5340--07-10,147

RF Design for Tactical Ultra-Light Unmanned Aerial Vehicle Radar System

JIMMY O. ALATISHE
ERIC L. MOKOLE
SUKOMAL TALAPATRA

*Surveillance Technology Branch
Radar Division*

LAWRENCE M. LEIBOWITZ
*SFA, Inc.
Crofton, MD 21114*

March 29, 2007

REPORT DOCUMENTATION PAGE

Form Approved
OMB No. 0704-0188

Public reporting burden for this collection of information is estimated to average 1 hour per response, including the time for reviewing instructions, searching existing data sources, gathering and maintaining the data needed, and completing and reviewing this collection of information. Send comments regarding this burden estimate or any other aspect of this collection of information, including suggestions for reducing this burden to Department of Defense, Washington Headquarters Services, Directorate for Information Operations and Reports (0704-0188), 1215 Jefferson Davis Highway, Suite 1204, Arlington, VA 22202-4302. Respondents should be aware that notwithstanding any other provision of law, no person shall be subject to any penalty for failing to comply with a collection of information if it does not display a currently valid OMB control number. **PLEASE DO NOT RETURN YOUR FORM TO THE ABOVE ADDRESS.**

1. REPORT DATE (DD-MM-YYYY) 29-03-2007		2. REPORT TYPE Formal		3. DATES COVERED (From - To)	
4. TITLE AND SUBTITLE RF Design for Tactical Ultra-Light Unmanned Aerial Vehicle Radar System				5a. CONTRACT NUMBER	
				5b. GRANT NUMBER	
				5c. PROGRAM ELEMENT NUMBER	
6. AUTHOR(S) Jimmy O. Alatishe, Eric L. Mokole, Sukomal Talapatra, and Lawrence M. Leibowitz*				5d. PROJECT NUMBER	
				5e. TASK NUMBER	
				5f. WORK UNIT NUMBER	
7. PERFORMING ORGANIZATION NAME(S) AND ADDRESS(ES) Naval Research Laboratory 4555 Overlook Ave., SW Washington, DC 20375-5320				8. PERFORMING ORGANIZATION REPORT NUMBER NRL/FR/5340--07-10,147	
9. SPONSORING / MONITORING AGENCY NAME(S) AND ADDRESS(ES) Office of Naval Research One Liberty Center 875 North Randolph Street, Suite 1425 Arlington, VA 22203				10. SPONSOR / MONITOR'S ACRONYM(S) ONR	
				11. SPONSOR / MONITOR'S REPORT NUMBER(S)	
12. DISTRIBUTION / AVAILABILITY STATEMENT Approved for public release; distribution unlimited.					
13. SUPPLEMENTARY NOTES *SFA, Inc., 2200 Defense Highway, Suite 405, Crofton, MD 21114					
14. ABSTRACT The Radar Division of the Naval Research Laboratory (NRL) has developed the radio frequency (RF) section of an unmanned aerial vehicle (UAV) radar system in support of the Navy's Tactical Ultra-Light (TUL) UAV program. This RF section consists of a local oscillator (LO) and timing-circuitry module, transmit and receive modules, and a calibration network. The objective of the UAV Radar project was to develop and demonstrate the feasibility of a target detection concept for the TUL UAV system. This concept includes hardware and digital signal processing (DSP) algorithms for target detection in high clutter and foliage with low false-track rates. The hardware effort described represents a significant contribution to the Navy's ability to field a TUL UAV system with an effective radar capability.					
15. SUBJECT TERMS Unmanned aerial vehicle (UAV) radar Receive module Transmit module Tactical Ultra-Light (TUL) RF section LO and timing-circuitry module Digital signal processing (DSP) Calibration network Field programmable gate array (FPGA)					
16. SECURITY CLASSIFICATION OF:			17. LIMITATION OF ABSTRACT	18. NUMBER OF PAGES	19a. NAME OF RESPONSIBLE PERSON
a. REPORT	b. ABSTRACT	c. THIS PAGE			Jimmy Alatishe
Unclassified	Unclassified	Unclassified	Unlimited	33	19b. TELEPHONE NUMBER (include area code) 202-404-5341

CONTENTS

1. INTRODUCTION	1
2. BACKGROUND	2
3. AIRBORNE PLATFORM DESIGNS	2
3.1 Helicopter Design	2
3.2 Aircraft Design	5
4. TRUCK-MOUNTED SYSTEM	5
4.1 RF Section	5
4.1.1 Transmit and Receive Module Frequency Plan	7
4.1.2 RF Implementation	8
4.1.3 Transmit Module	9
4.1.4 Receive Module	11
4.1.5 Receive Module Signal-Calibration Card	13
4.1.6 Calibration Network	14
4.1.7 LO and Timing-Circuitry Module	14
5. MEASUREMENTS AND RESULTS	15
5.1 Transmit Module	15
5.2 Receive Module	18
6. SUMMARY AND CONCLUSIONS	26
7. ACKNOWLEDGMENTS	26
REFERENCES	27
ABBREVIATIONS AND ACRONYMS	27

FIGURES

Fig. 1 — Block diagram of helicopter UAV design	3
Fig. 2 — Antenna section design for helicopter, aircraft, and truck-mounted systems	4
Fig. 3 — Block diagram of aircraft-mounted UAV system	6
Fig. 4 — Simplified block diagram of the RF section of the truck-mounted demonstration system	6

Fig. 5 — Final design for the UAV radar radiation aperture	7
Fig. 6 — General block diagram of the transmit module	10
Fig. 7 — Photograph of transmit-module prototype.....	11
Fig. 8 — General block diagram of the receive module of the truck-mounted system	12
Fig. 9 — Photograph of the receive-module prototype.....	12
Fig. 10 — Receive-module signal-calibration card	13
Fig. 11 — Photograph of receive-module signal-calibration-card prototype	13
Fig. 12 — LO and timing-circuitry module.....	14
Fig. 13 — Testbed for the characterization of the transmit module	16
Fig. 14 — Output spectrum of the combined transmit module/power amplifier.....	17
Fig. 15 — Output spectrum of the transmit module/power amplifier combination using an LFM chirp with 0-dBm peak power as the input signal	17
Fig. 16 — Testbed for the characterization of the receive module	18
Fig. 17 — Spectrum of the radar receiver first LO with 2215-MHz F_c and 13-dBm peak power level	19
Fig. 18 — Spectrum of the radar receiver second LO with 960-MHz F_c and 13-dBm peak power level ..	19
Fig. 19 — Spectrum of input signal used to measure gain and NF of the radar receiver	20
Fig. 20 — Spectrum of receive module output signal used to measure gain and NF of radar receiver.....	21
Fig. 21 — Gain curve of the receive module.....	21
Fig. 22 — Spectrum of the input signal used to measure the SFDR of the receive module.....	22
Fig. 23 — Output spectrum of the receive module produced by the 1300-MHz input signal.....	23
Fig. 24 — Testbed setup for the two-tone test used to determine the second-order IMD ratio for the receive module	24
Fig. 25 — Spectrum analyzer image of the input spectrum used in the two-tone test for the receive module.....	24
Fig. 26 — The output spectrum used in the two-tone test for the receive module	25

TABLES

Table 1 — Transmit and Receive Module Frequency Plan	8
Table 2 — Transmit and Receive Module Specifications	9
Table 3 — LO and Timing-Circuitry Module Specification	14
Table 4 — Transmit Module Calculated and Measured Parameter Results	18
Table 5 — Receive Module Calculated and Measured Parameter Results.....	26

RF DESIGN FOR TACTICAL ULTRA-LIGHT UNMANNED AERIAL VEHICLE RADAR SYSTEM

1. INTRODUCTION

The Radar Division of the Naval Research Laboratory (NRL) has developed the radio-frequency (RF) section of an unmanned aerial vehicle (UAV) radar system [1]. This effort was in support of the Navy's Tactical Ultra-Light (TUL) UAV Program sponsored by NAVAIR PMA-263. The RF portion of the system consists of a local-oscillator (LO) and timing-circuitry module, transmit and receive modules, and a calibration network.

The objective of this UAV Radar project was to develop and demonstrate the feasibility of a radar concept and associated hardware and digital signal processing (DSP) algorithms that could be applied to the TUL UAV Program. Major features of this radar include the following capabilities:

1. Detect slowly moving targets in high, stationary clutter environments;
2. Provide a synthetic aperture radar (SAR) map of the ground;
3. Provide some degree of detection of moving targets covered by foliage using various algorithms like Velocity SAR (VSAR) [2], Displaced Phase Center Antenna (DPCA) [3], and Space Time Adaptive Processing (STAP) [1]; and
4. Provide low false-track rates.

Such a radar will allow the Navy to detect over-the-horizon targets, cue weapons against slowly moving targets, and detect targets within three specific range-resolution cells of 50, 75, and 100 ft associated with the 1 to 15 kft range of flying altitudes of the TUL UAV.

The radar constructed is a low-power (300 W peak, expandable to 1 kW), L-band (1215 to 1400 MHz) system that is capable of detecting small targets out to an unambiguous range of 25 nmi, which is expandable to 80 nmi. The radar's pulse repetition interval (PRI) is tunable to about 1 ms, with corresponding pulse repetition frequency (PRF) of 1 kHz, which gives it the ability to meet the range specification. The antenna array is partitioned into two segments that are separated by an isolation surface. It consists of a transmit planar array of four identical, parallel, 13-dB gain, center-fed dipoles with a backplane and a receive array of 24 center-fed, vertically polarized, microstrip dipoles. To provide the desired range resolution, the radar transmits band-limited signals over the three bandwidths of 1, 7.5, and 10 MHz. When the radar return signal is detected, it is converted to a baseband signal, which is digitally stored for offline processing. To permit the detection of low-power (-90 dBm) 13-dB signal-to-noise ratio (SNR) signals, each receiver channel has a total gain of 50 dB and a noise figure (NF) of 6 dB with a spur-free dynamic range (SFDR) of 80 dB. The weight objective of this radar design was less than 300 lb in order to meet the TUL UAV testbed payload specification. It has been estimated that an operational implementation would require a radar payload limit of less than 150 lb.

Although the radar's intended platform, a Vertical Tactical UAV (VTUAV), is small, this program used a truck-mounted system to test the viability of the concept and design. To simulate the motion and geometry of a VTUAV, the truck-mounted system was situated in elevated areas of western Maryland overlooking low-lying roads. A moving test target (a truck with a corner reflector) at various velocities was situated at several designated locations along these roads. The radar platform (truck) was positioned at a range of 1 to 4 nmi at an elevation of approximately 1,000 ft above the target. The route of the radar platform moving at a velocity of 40 mph, to secure the requirement for velocity resolution, was placed along a parallel path to the target. As the platform moved, the radar transmitted various signals and collected data. Following completion of the experiment, the data were analyzed to determine whether the simulated target had been detected. The focus of this report is the RF design and not the radar performance, which is addressed in Ref. 4.

Section 2 of the report provides a brief background of the VTUAV including design perspectives, major design modifications, and reasons for those modifications. Section 3 describes the designs considered for the various platforms. Section 4 addresses the RF design for the truck-mounted system and each of the modules. A brief discussion of the radar is presented and is followed by a description of the transmit, receive, and LO and timing-circuitry modules and calibration network. This includes the operation, design topology for the transmit and receive modules as well as the expected performance of each module. A major challenge in designing and building the TUL UAV Radar was the need for small, low-cost, lightweight modules. Commercial-off-the-shelf (COTS) cellular-phone components were found to be a viable design solution due to their low cost, performance, reliability, and small packaging. The resulting module designs provide straightforward implementation with minimal risk of failure. Section 4 also describes the steps taken to use these components in developing a radar that could provide for the transmission and reception of band-limited signals with very low phase noise. In Section 5, measured data obtained from the modules and the radar are presented and discussed. Finally, Section 6 provides a brief summary of the development and test results as well as future applications.

2. BACKGROUND

The design of a VTUAV radar must, of course, consider the UAV platform. Unfortunately, the unavailability of a VTUAV for this program necessitated the identification of appropriate testbed platforms that could mimic the performance of the intended platform. Consequently, designs were developed for three different testbed platforms: a helicopter; an airplane; and a utility truck. The key factors in each design were cost, ease of use, and speed of construction. All three platform designs had the functionality and ability to emulate the performance of a VTUAV. However, because the costs of flight certification and the retrofit of the laboratory antenna array for each airborne platform were prohibitive relative to the cost constraints of the program, the utility truck was selected as the vehicle of choice. Brief descriptions of each design are presented below.

3. AIRBORNE PLATFORM DESIGNS

3.1 Helicopter Design

The helicopter design, as shown in Fig. 1, has two basic components, the antenna section and the control system section. The antenna section consists of a transmit array, a receive array, and a calibration network, which are separated by aluminum isolation barriers. The control system section consists of a control computer with manual control, navigation, and data storage inputs and a frequency sources module. The frequency sources module provides required frequency signals to both the control system and antenna sections. Control system data are presented to the antenna section through a field programmable gate array (FPGA) via a fiber-optic (FO) link.

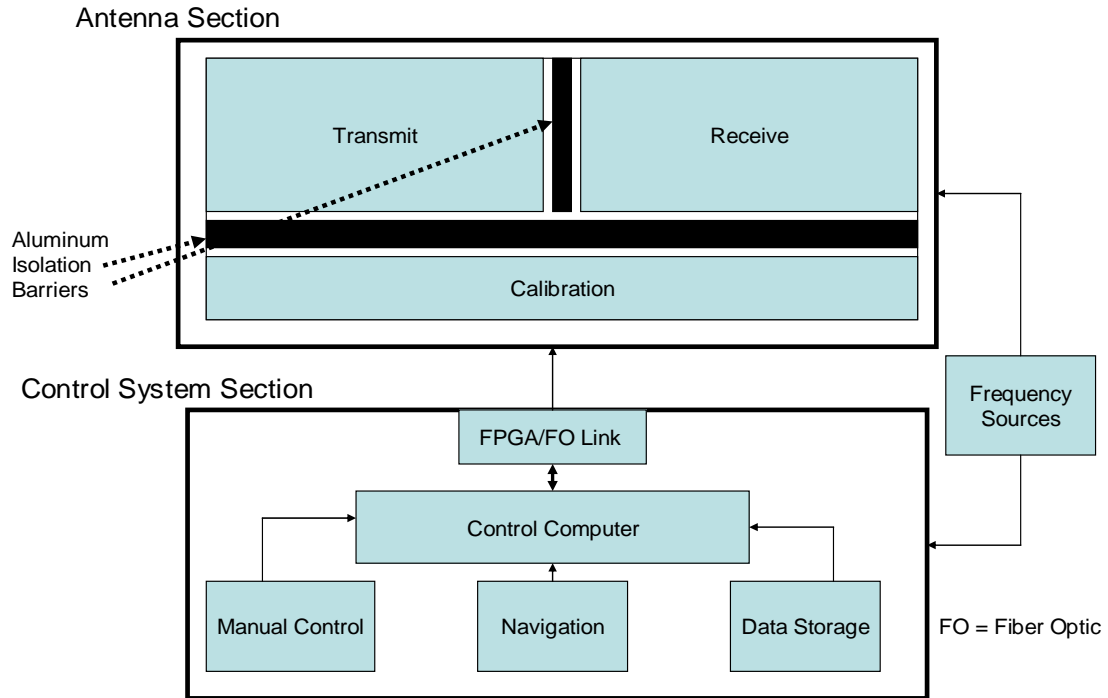


Fig. 1 — Block diagram of helicopter UAV design

As shown in more detail in Fig. 2, the primary components of the antenna section are the transmit and receive arrays. The transmit array consists of a four-element planar array of parallel dipoles, four power amplifiers, and four transmit modules. The dipoles are center-fed and equally spaced, with half-wavelength interelement separation between the feeds in both directions as indicated in Fig. 2. Each dipole is fed by a power amplifier of an exciter upconverter (transmit module), which is in turn fed by an FPGA waveform generator/digital-to-analog converter (DAC) via an FO link. The waveform generator produces a band-limited signal at an intermediate frequency (IF). This band-limited signal is fed to the transmit module, which upconverts the spectrum of the band-limited signal to the radar's operating band. The power amplifier provides a signal at the correct power level for free-space transmission.

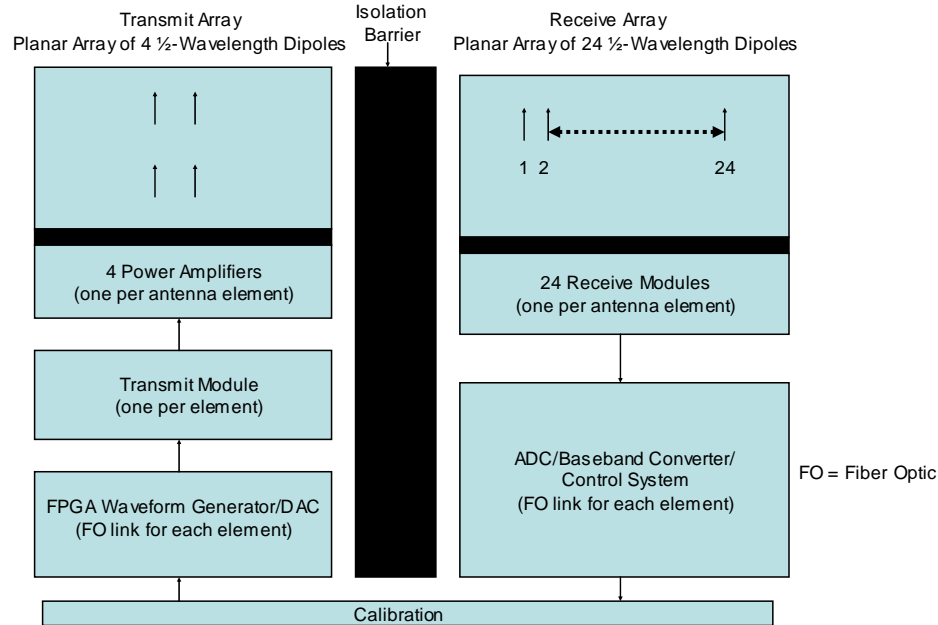


Fig. 2 — Antenna section design for helicopter, aircraft, and truck-mounted systems

The receive array is an aggregate of individual, vertically polarized, microstrip dipole elements that are used in a SAR mode. The receive array includes 24 center-fed elements and is separated from the transmit array by an aluminum isolation barrier. Each antenna element feeds a receive module/downconverter, which then feeds an analog-to-digital converter (ADC)/digital baseband converter in the control system section. When the receive array senses the RF energy return scattered from a target, the RF signal from each receive element is downconverted to an IF for digital processing. The downconverted signal is sent to the DSP section for baseband conversion, data collection, and digital post-processing including the STAP, VSAR, and DPCA algorithms. (For explanations of these algorithms see Refs. 1, 2, and 3, respectively). The 24 array elements, with interelement horizontal quarter-wavelength separation and interelement vertical half-wavelength separation, were spaced to match the velocity of a moving platform along with the PRI for each return pulse from the target. This is also a requirement for the DPCA (VSAR) algorithm in order to establish the velocity resolution.

The calibration network of the antenna section, shown in both Figs. 1 and 2, is needed to remove any signal anomalies created by the system. It consists of an integrated system of switches and directional couplers that direct a test signal from any one of the four transmitters and back into all of the receiver elements. The switches are computer controlled via FO links to provide the user with the ability to perform a full-scale in-flight radar calibration at any time during an experiment or other operation.

The control system section design, as shown in block diagram form in Fig. 1, is essentially the same for the helicopter, airplane, and truck platforms. The subsystems consist of a manual control unit, a navigation unit, a data storage unit, a control computer, a frequency sources module, and FO interfaces for the transmit and receive modules and calibration network. The FO interfaces provide optical signals from the control computer to the various parts of the system in order to provide synchronization for a given operation. These control signals select the waveform, PRI/PRF, system operating modes, etc. In addition to automatic control, the manual control unit allows the user to manipulate the entire radar system while the platform is in flight. The storage unit, consisting of an assortment of data buses and digital storage media, is activated when it is necessary to collect data. Once the signal returns are pre-processed, the data are sent and stored in the data storage unit. The navigational unit, which contains the

GPS module and the inertial navigation unit, sends information to the data storage unit for time-stamping and adding location markers to the collected data. The clock and LO signals are generated and distributed by the frequency sources module. The signals generated by the frequency sources module synchronize the radar system, thereby ensuring pulse-to-pulse phase coherency. The control system section design is not discussed here in further detail since the focus of this report is the RF design.

3.2 Aircraft Design

The second testbed design considered an airplane as the intended radar platform, which required several modifications to the original helicopter design. These changes included reducing the number of receiver antenna elements from 24 to 16 (four elements minimum), reducing the number of transmit modules from four to one, and simplifying the calibration network. These changes reduced the size, cost, and complexity of the testbed radar. A block diagram of the aircraft-mounted UAV system is shown in Fig. 3. To illustrate the simplification in the calibration network, the path of a calibration signal is explained in the following description. The CW calibration signal created by the waveform generator passes through a switch that disconnects the transmit module from the power amplifier to prevent the radar from radiating the signal. The calibration signal is directed to a directional coupler to attenuate the signal that passes through the coupled port. The calibration signal is then directed through another switch that decouples the receive array from the receive modules. By means of a 2:1 switch, the resulting signal is then used to set the system to one of two modes of operation, either a stand-down (calibration) mode or a radar-operation mode. Finally, a 16:1 signal splitter distributes the calibration signal to the receive modules. The signal is then sent to the data storage unit for comparison with actual radar data. Further discussion of the calibration network is presented in Section 4.1.6.

4. TRUCK-MOUNTED SYSTEM

A truck with a temperature-controlled shelter was selected as the radar platform for the demonstration system and the radar was constructed based on the aircraft design discussed above. Consequently, the associated radar is essentially equivalent to the aircraft design of Fig. 3 but with some minor modifications. The various components of the truck-mounted radar system are described below.

4.1 RF Section

As shown in the simplified block diagram of Fig. 4, the RF section of the demonstration system includes the Antenna Section and the LO and timing-circuitry module. The antenna section consists of a transmit module, a power amplifier, a 4:1 splitter, four (extendable to 16) receive modules, and a calibration network. The LO and timing-circuitry module primarily consists of a crystal reference, three phase-locked loops (PLLs), and an HP frequency synthesizer. The functions of the RF section are summarized here and addressed in more detail later in this section of the report. The transmit and receive modules and calibration network are located behind the antenna elements in their respective panels in the UAV radar radiation aperture structure shown in Fig. 5. The transmit-side antennas consist of an array of four center-fed planar dipole elements with half-wavelength horizontal and vertical spacing. These elements are driven by a single power amplifier using a 4:1 power splitter. The function of the transmit module is to upconvert a linear-chirp signal, while simultaneously providing sufficient output power and SFDR. The output of the transmit module drives the power amplifier. This output signal must be at least 7.5 dBm with an SFDR of at least 80 dB in order to provide sufficient drive to the power amplifier and prevent it from producing intermodulation distortion (IMD) signal products, which can cause interference with other RF systems and potentially create false targets and/or alter range-time sidelobe performance.

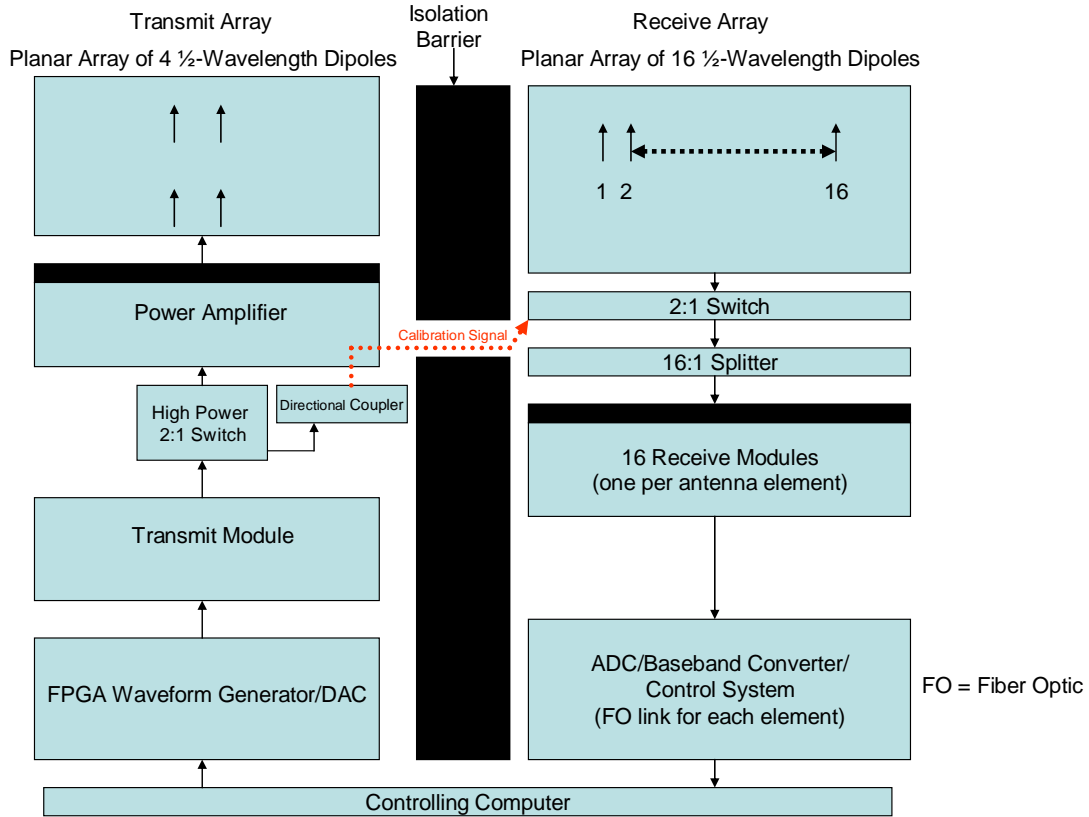


Fig. 3 — Block diagram of aircraft-mounted UAV system

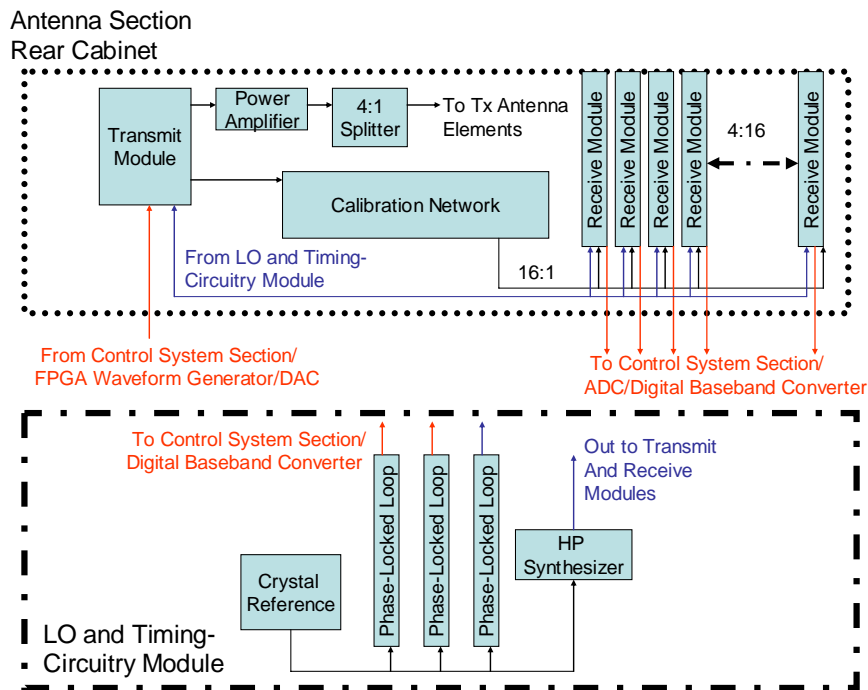


Fig. 4 — Simplified block diagram of the RF section of the truck-mounted demonstration system

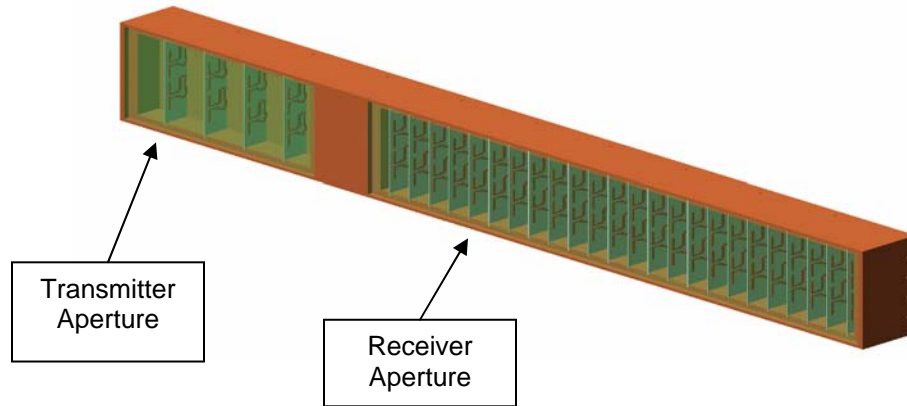


Fig. 5 — Final design for the UAV radar radiation aperture

The FPGA waveform generator in Fig. 3 provides a linear chirp with a center frequency (F_c) of 45 MHz and an instantaneous bandwidth ranging from 1 to 10 MHz at the input port of the transmit module shown in Fig. 4. The signal is then amplified, filtered, and frequency-converted by a mixer to a UHF IF. The IF signal is processed in a similar manner by converting it into an L-band signal at a nominal frequency of 1300 MHz. The L-band signal is in turn filtered, amplified, fed to the power amplifier, and then radiated into space via a 4:1 splitter and the transmit antenna elements.

When the radiated signal illuminates a target, the resulting monostatic scattered field return at L-band impinges on the receiver array of four planar dipole elements with quarter-wavelength horizontal spacing. The received RF signal is fed to the input port of a receive module. The receive modules employ the same components as the transmit module with the addition of a low-noise amplifier (LNA). Amplifying and frequency shifting the received signal twice results in a signal at an IF of 45 MHz. These signal outputs from the receive module are then fed to the baseband converter for digital pre-processing.

The calibration network consists of a directional coupler that is connected to the input port of the power amplifier, a switch, and a 4:1 power splitter that is connected to a switch nested in the receive module. The calibration network characterizes both the transmit signal and receive channels in order to maintain received amplitude and phase purity by equalization. The output of the transmit module is sampled and sent to all the receive modules for offline recording by the control system section. By this method, each of the receive channels is first adjusted offline to make it homogeneous in amplitude and phase. The recorded signal is then compared offline to the original transmit excitation signal and a new excitation signal is formed and generated. The resulting transmitted signal equalizes out phase and amplitude anomalies produced by the systems in a one-time non-real-time calibration.

The LO and timing-circuitry module of Fig. 4 consists of a 10-MHz crystal oscillator reference, three PLLs, and an HP frequency synthesizer plus an assortment of other components including amplifiers, attenuators, and power splitters. Much lighter and smaller equipment than the HP synthesizer would be used in an operational system implementation. Each PLL and the frequency synthesizer are locked to the 10-MHz reference so that the resulting clock signals and first and second LOs are also locked to the reference and the entire radar is thus phase coherent.

4.1.1 Transmit and Receive Module Frequency Plan

The transmit and receive module frequency plan is shown in Table 1. The reasons for selecting this frequency plan are that: (1) it permits the use of a superheterodyning technique called “high-side frequency conversion,” and (2) these frequencies, except for 1215 to 1400 MHz, are common to the communications industry for which components are readily available. The phrase “high-side frequency

conversion” is defined as using an LO frequency higher than the RF frequency, in a mixer, instead of using RF and LO signals very close in frequency to achieve the IF. Using this approach, the higher-order IMD products are greatly attenuated, thereby reducing any potential signal interference.

Table 1 — Transmit and Receive Module Frequency Plan

Function	IF 1 (MHz)	IF 2 (MHz)	IF 3 (MHz)	LO 1 (MHz)	LO 2 (MHz)
Transmit	45	915	1215 to 1400	960	2130 to 2315
Receive	1215 to 1400	915	45	2130 to 2315	960

4.1.2 RF Implementation

4.1.2.1 Components

Surface mount technology or monolithic microwave integrated circuits (MMICs) were used to develop the transmit and receive modules for the UAV radar. MMICs are very small components that are soldered directly to the surface of a printed circuit board (PCB). A design employing this technology was selected to achieve the required specifications. The proper components, including amplifiers, filters, mixers, resistors, etc., were chosen to realize the design and achieve anticipated system performance. The next phase was to design a PCB layout for each component, construct prototype circuits, and then mount, test, and characterize each of them. These prototype boards were assembled in the form of a brassboard (testbed) into either a transmitter or receiver topology, as appropriate, and then characterized and optimized in order to construct a final PCB design. The final design was tested and then integrated into the overall radar design.

In developing the transmit and receive module brassboards, the relative proximity to other components required special attention. For example, amplifier circuits that are too close to one another can cause RF coupling, which can lead to spurious activity or free-running oscillations in the spectrum of operation of the modules. Though the real estate of the transmit and receive module testbed could be as large as necessary, the final design of the prototype modules had to be confined within a PCB area of 4.5 in. by 15 in. and nominal height of less than 1.0 in. As a result, the oscillations are sufficiently suppressed with proper isolation between stages within the modules. Also, the proper selection of PCB substrate was essential. This choice basically determined the overall size of the module since dielectric constant and conductor line width are related for most high-frequency PCB topologies. Depending on the selection, these substrates can be very expensive with respect to their material properties. Roger’s Corporation SuperLam 2000 ($\epsilon_r = 2.54$), which is a very flexible material, was chosen for this design. An overview of the topology of the modules and expected performance is presented in the next section. It has been estimated that an operational TUL UAV radar implementation would require modules limited to a weight of less than 8 oz with a PCB area of no more than 4 in. by 6 in. and height of no more than 1.0 in.

4.1.2.2 Coplanar Waveguides

The design and layout of the transmit and receive modules use grounded coplanar waveguide topology. A grounded coplanar waveguide consists of three metal conductors (a center conductor line or RF path separated by a gap on either side met by ground planes) on the surface, a ground plane on the bottom, and a dielectric medium set in between them. This topology is useful for active devices due to the location of the input/output leads of the device and the close proximity of the ground plane to the grounding terminals on either side. This topology is also useful in minimizing RF coupling between stages, which is primarily attributed to the nature of the electric field terminating at ground planes parallel to the RF path. The geometry of this layout supports even and odd quasi-transverse electromagnetic (TEM) modes, which provide efficient transmission. This results in low-loss propagation at high

frequencies along the RF path and, in some instances, minimal stray radiation, which is one of the causes of RF coupling between active and passive components.

A TEM mode is described as an electromagnetic (EM) guided wave (homogenous) that has neither an electric nor magnetic field component in its direction of propagation. In order for this mode to exist in the waveguide, a homogeneous dielectric layer is required to exist throughout and around the geometry. The prefix “quasi” would imply the nonhomogeneous nature of the electric field due to the discontinuities in the dielectric medium encompassed by the two metal layers, i.e., the air surrounding the two metal layers and the dielectric between them. The terms even and odd refer to the orientation of the electric field in the gaps separating the center conductor from the ground planes (same orientation for even and vice versa for odd) [5]. For the purposes of this design, a characteristic impedance of 50Ω was required for the optimum performance of all the components. This impedance was achieved by using coplanar waveguide impedance formulas [5]. These formulas relate the line (characteristic) impedance to the type of dielectric (between the metal layers), its height, the width of the center conductor line, and the total width of the gaps between the center conductor line and the ground planes on either side.

4.1.3 Transmit Module

Based on spreadsheet calculations using individual RF component characteristics, the specifications for the transmit and receive modules, including gain, NF, SFDR, and third-order intercept (TOI) point, are shown in Table 2. The goal of the current module designs was to meet these specifications.

Table 2 — Transmit and Receive Module Specifications

Module	Gain (dB)	NF (dB)	SFDR (dB)	TOI (dBm)
Transmit	10.0	N/A	80.0	37.8
Receive	24.6	6.0	80.0	21.2

A block diagram of the transmit module is shown in Fig. 6. The transmit module consists of an IF Surface Acoustic Wave (SAW) filter with an F_c of 45 MHz and an input bandwidth of 10 MHz. A SAW filter has the ability to provide an almost ideal frequency selectivity within a small package. However, these components are not without limits. This filter has an insertion loss of about 25 to 27 dB due to the relationship between percentage bandwidth and its physical size. The next component in the circuit path is the amplifier, which is the only type of amplifier used in the design of the transmit and receive modules. It operates within the frequency band from DC to 4 GHz, has a gain of 17.4 dB, a NF of 4.1 dB, and a 1-dB compression point (P1dB) of about 19.6 dBm referenced to the output. This amplifier is used to recover some of the signal power needed in the next section of the circuit.

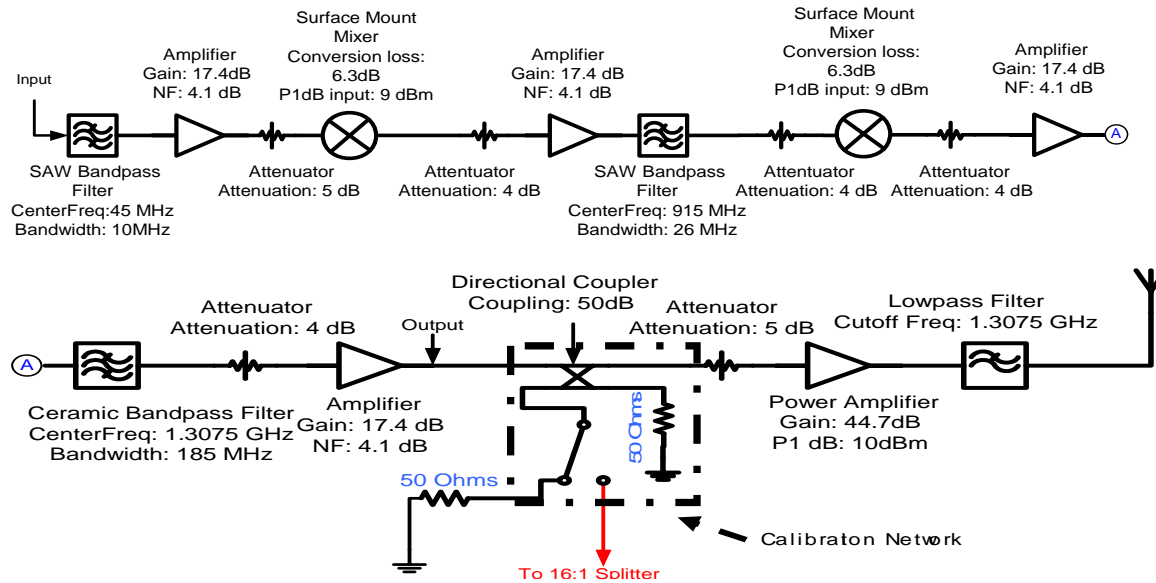


Fig. 6 — General block diagram of the transmit module

A mixer with a 5-dB attenuator for input protection is used for frequency conversion. It has a conversion loss of approximately 6.3 dB (depending on how the part is mounted) and its measured RF-to-LO and LO-to-RF isolation is normally about 25 dB. For simplification of the block diagram, the LOs are not shown in Fig. 6. With the first LO signal at 960 MHz, the IF is translated in frequency from 45 MHz to 915 MHz. This signal is then attenuated by 4 dB and amplified to recover signal strength and it is then filtered by another set of SAW filters. The configuration consists of two SAW filters of the same manufacturer, with an F_c of 915 MHz and bandwidth of 26 MHz (connected by a 1-dB attenuator). Each filter has an insertion loss of about 3 dB in the passband with about 36 dB of loss over the frequencies of 940 to 970 MHz. A single filter could not provide sufficient attenuation of the LO signal, which is coupled over in the signal path, and other unwanted signals (like harmonics or IMD products from the mixers). Thus, two SAW filters were required along with an attenuator (pad) for matching the input and output impedances of the filters.

Once this signal is selected in frequency by the two SAW filters and attenuated by a 4-dB pad to protect the next stage, it is again frequency translated by another mixer of the same model. The LO of this mixer can be tuned to any frequency within the range of 2130 to 2315 MHz. This capability should place the signal in the appropriate radar frequency band (L-band). Next, the signal is passed through a 4-dB pad, amplified, and filtered by a ceramic bandpass filter containing six dielectric resonators. This filter has a 3-dB passband of 185 MHz with an F_c of 1307.5 MHz (L-Band) and an insertion loss of 2 dB. The output of the filter is attenuated by a 4-dB pad and amplified to provide adequate power at the output of the transmit module.

The transmit module output signal is then sent to a directional coupler that sends the signal via the direct path to a connectorized 5-dB pad (which is optional depending on the transmit module output power), class-C amplifier, and a 4:1 splitter embedded in the transmit array. The signal is also sent via the coupled path through a 2:1 switch and then either to a termination to ground or a 16:1 splitter for use by the calibration network. The class-C power amplifier is tuned to operate at L-band. It takes a pulsed signal at a typical peak input power level of 10 dBm and delivers 300 W (peak) at the output. The average output power depends on the input signal duty factor (e.g., the 10% duty factor used in this application produces an average output power of 30 W). The high-power, co-axial, low-pass filter (LPF) is used to suppress the harmonics produced by the power amplifier. Each output of the 4:1 splitter in the transmit

array is sent to a vertically polarized dipole that converts the RF signal to a radiated signal. A photograph of the transmit module prototype is shown in Fig. 7.

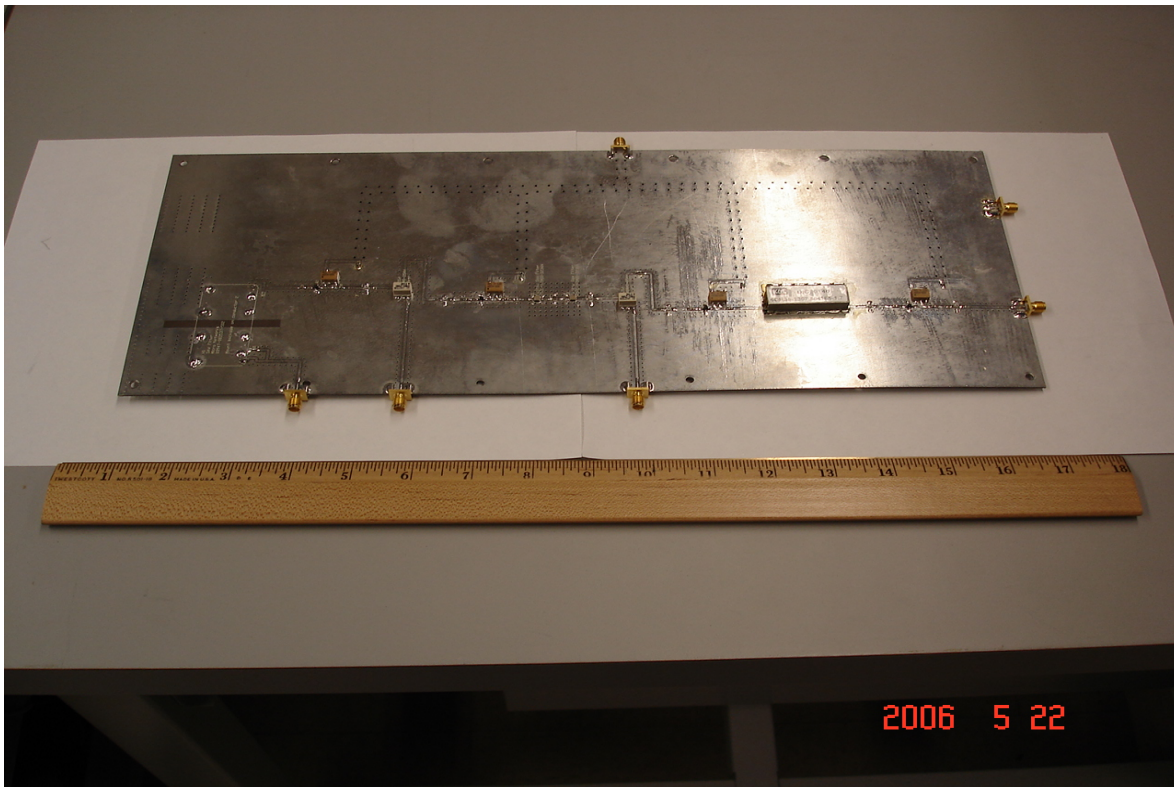


Fig. 7 — Photograph of transmit-module prototype

4.1.4 Receive Module

The receive module specifications are also provided in Table 2. A block diagram of the receive module of the demonstration system is shown in Fig. 8 where again for simplification the LOs are not shown. With the transmitted radar signal reflected by an object in space, the echo is returned to the receive aperture. Each receiver radiating element is connected to the receive modules by a transistor-to-transistor logic (TTL) blanking switch, which provides 40-dB (minimum) suppression of the coupled transmitted signal power and a limiter that protects the receiver by limiting the amount of receive power to 6 dBm (13 dBm maximum). The signal is then propagated through the receive module in a manner similar to that of the transmit module, but inverted. The signal is presented to the receive module through a 2:1 switch with a path either directly from the receive antenna or from a calibration signal source via a 20-dB attenuator. An LNA, with the same properties of those used in the transmitter, amplifies the signal and sets the NF. This signal is attenuated by a 5-dB pad, then amplified by a similar amplifier, and filtered by a ceramic bandpass filter (the same type of component used in the transmit module). Once the signal is filtered in the L-band frequency range, it is attenuated and downconverted to an F_c of 915 MHz. The same manner of filtering, attenuation, amplification, and filtering occurs, and then the signal is again mixed down to an IF of 45 MHz. The resulting signal is attenuated, amplified, filtered, amplified again, and then sent to the signal-calibration card. The purpose of the signal-calibration card is to ensure that within 10 MHz of bandwidth, the receiver output noise power level is greater than the noise level of the DSP unit ADC. A photograph of the receive module prototype appears in Fig. 9.

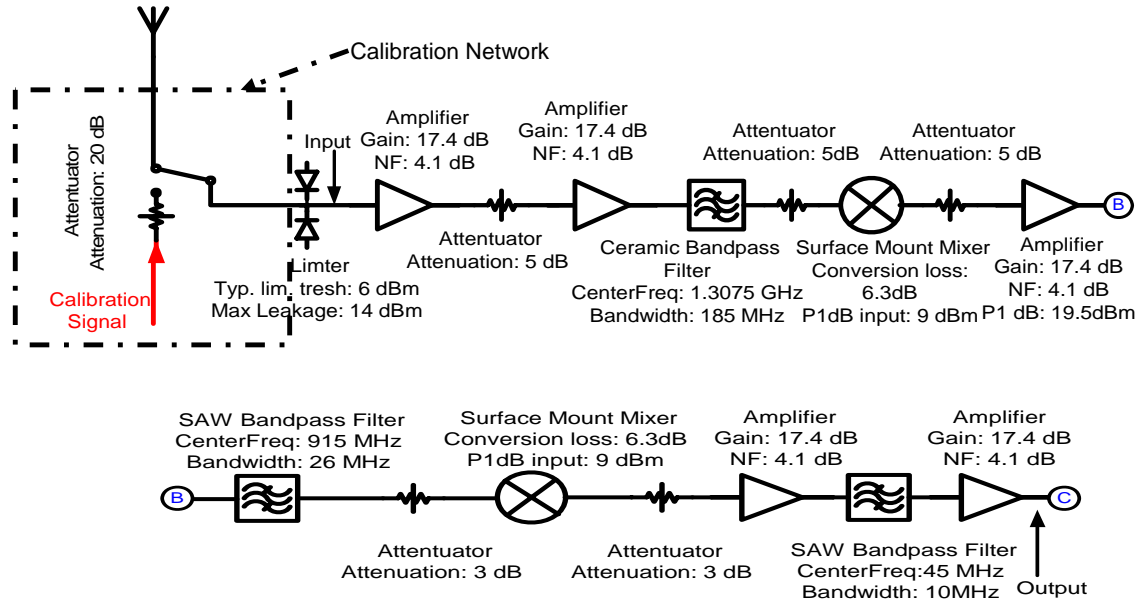


Fig. 8 — General block diagram of the receive module of the truck-mounted system

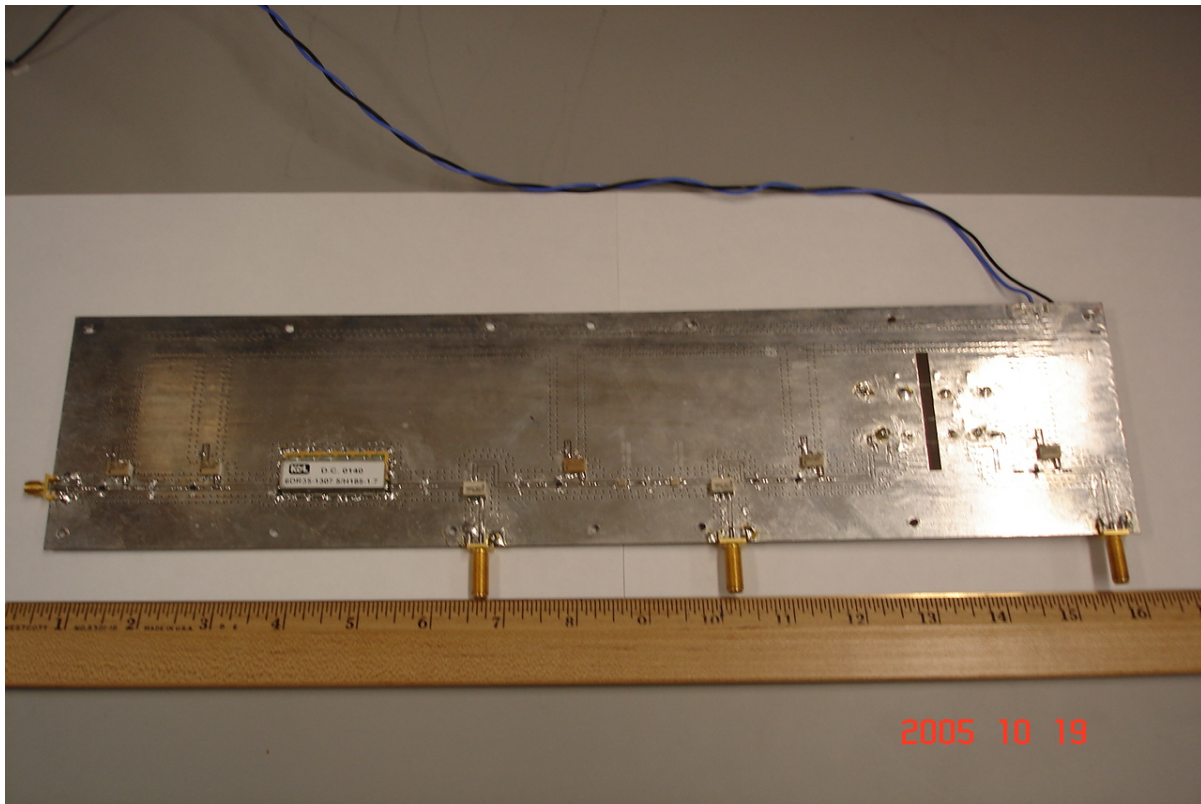


Fig. 9 — Photograph of the receive-module prototype

4.1.5 Receive Module Signal-Calibration Card

The signal-calibration card shown in the block diagram of Fig. 10 contains an optional external pad, an attenuator, an amplifier similar to those used in the transmit and receive modules, an attenuator, a clamping amplifier to protect the ADC and amplify the signal, and finally an LPF with an F_c of 70 MHz and insertion loss of 1.2 dB to suppress the harmonics produced by the clamping amplifier. The analog signal output of the filter is converted to a digital signal, processed, and then stored for offline processing. A photograph of the receive module signal-calibration card prototype appears in Fig. 11.

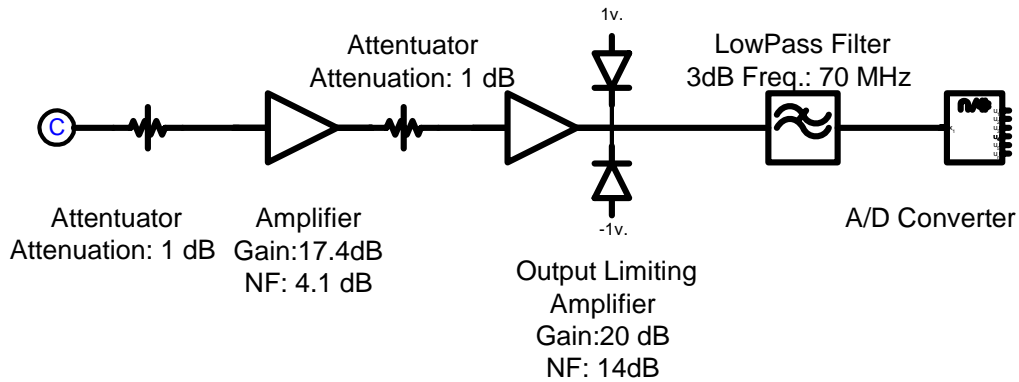


Fig. 10 — Receive-module signal-calibration card

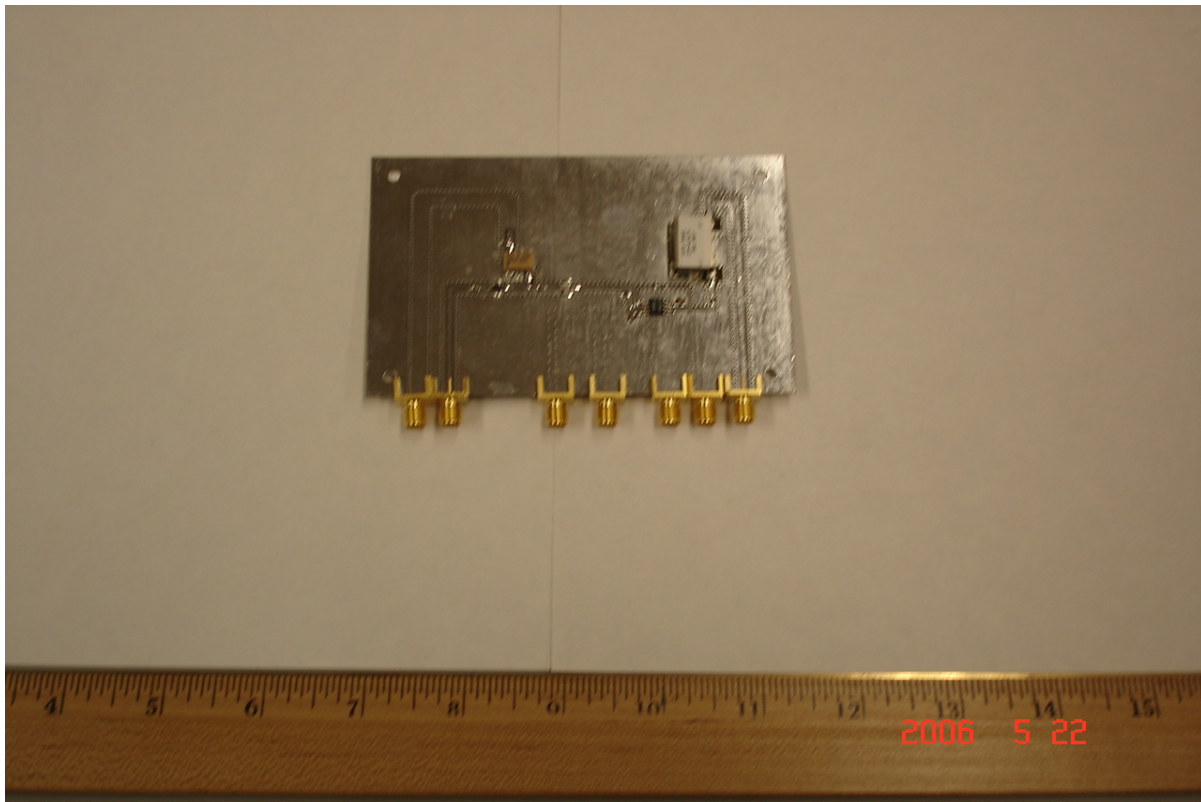


Fig. 11 — Photograph of receive-module signal-calibration-card prototype

4.1.6 Calibration Network

A switch that disconnects the transmit module from the power amplifier and a low-insertion-loss L-band 50-dB directional signal coupler are connected at the output of the transmit module, just before the power amplifier, in order to provide a very-low-power calibration CW signal to a 16:1 power splitter. The outputs of the 16:1 divider are each connected to the 16 receiver channels through 16 switches contained in the receive modules. This calibration signal is examined offline for amplitude and phase variations in all transmit and receive channels. Once this information is obtained, a new transmit waveform is developed with the amplitude and phase information from the calibration signal embedded in it. This is done in an attempt to make the receive channels nearly identical and the transmit waveform uncorrupted.

4.1.7 LO and Timing-Circuitry Module

As shown in Fig. 12, the LO and timing-circuitry module consists of a 10-MHz crystal oscillator reference, three phase-locked loops (PLLs), and an HP Agilent E8244A frequency synthesizer. For simplicity, other assorted components including amplifiers, attenuators, and power splitters are not shown. The 10-MHz crystal oscillator was selected in accordance with the specification requirements presented in Table 3. This component acts as the reference oscillator that drives the other signal sources and keeps them phase coherent. It has an output power level of 13 dBm but, followed by a 7-dB pad and a 4:1 splitter, it is well suited for use in driving the other sources. The reference oscillator signal is distributed to the three PLLs and the HP frequency synthesizer. Each of the PLLs is locked to the 10-MHz reference in order to provide clock signals at 60 MHz and 120 MHz and the second LO at 960 MHz, respectively. In addition, the first LO provided by the HP synthesizer is also locked to the reference so that the entire radar is phase coherent.

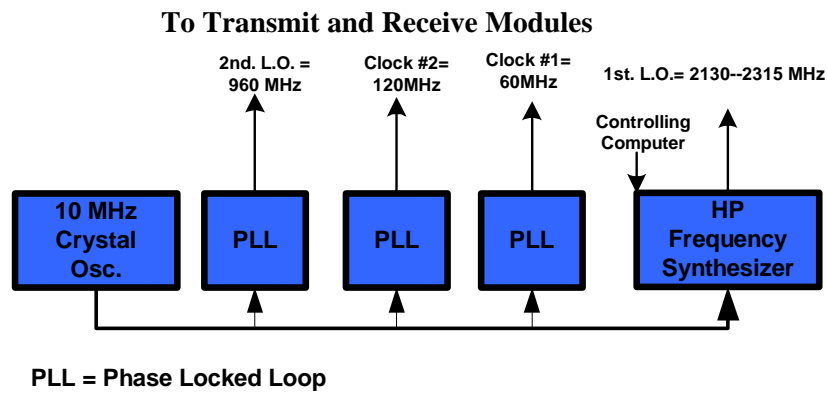


Fig. 12 — LO and timing-circuitry module

Table 3 — LO and Timing-Circuitry Module Specification

Signal Frequency	10 MHz	60 MHz	120 MHz	960 MHz	2130 to 2315 MHz
Phase Noise at 50Hz Offset from the Carrier	-145 dBc/Hz	-80 dBc/Hz	-80 dBc/Hz	-80dBc/Hz	-80 dBc/Hz
Output Power Level at 50 Ω	6 dBm	7 dBm	N/A	28 dBm	28 dBm

For the PLLs, the signals are produced with an output power of about 11.5 dBm. The 60-MHz source is fed through a 4:1 splitter and then distributed to the DSP console. The 120-MHz signal was originally intended for an older ADC but was not used. The 960-MHz signal is attenuated by a 10-dB pad and amplified so that the final signal strength is about 26 to 28 dBm. This signal is presented to a 16:1 splitter and then to the transmit and receive modules at the appropriate signal level (13 dBm) and used as the first LO. Finally, the 10-MHz reference is sent to the signal synthesizer. This tunable device has an external port that allows it to lock to an outside reference signal. The output power level for the synthesizer signal is adjustable to 30 dBm and is distributed and used in the same manner as the 960-MHz LO signal, allowing the modules to translate the 915-MHz signal to and from L-band.

5. MEASUREMENTS AND RESULTS

As stated above, the objective of the TUL UAV Radar project was to develop and demonstrate a feasible concept and DSP algorithms that would provide for the detection of targets in high clutter and foliage at required low false-track rates. A truck-mounted design was chosen to meet the requirements and simulate a UAV-mounted system and a prototype was constructed and tested. The calculated performance specifications of the transmit and receive modules are based on spreadsheet computations performed during the design phase using individual component characteristics. The testing included laboratory measurements performed on the prototype hardware to confirm that the calculated module operating performance specifications were achieved.

5.1 Transmit Module

As shown in the Antenna Section of Fig. 4, an FPGA Waveform Generator/DAC feeds a transmit module, which is followed by a power amplifier and then through a four-way splitter to four transmit array elements. Figure 13 is the block diagram of the testbed used to characterize the transmit module. Using this configuration, the gain and output power were determined. The input source provides a 45-MHz CW tone or a frequency-swept signal (chirp) with F_c of 45 MHz and BW of 10 MHz. Either signal has an instantaneous peak power level of 0 dBm. This is done to ensure that the transmit module with gain of 10 dB is operating in the linear region and that there is enough input signal to activate the power amplifier during testing. The signal is pulse modulated using a pin-diode modulator, which is a single-pole single-throw (SPST) switch. This is done because the power amplifier is a class-C amplifier, which in most cases can only accept signals with duty factors of $\leq 10\%$. The HP 8012B pulse generator that controls the SPST switch produces a 1-ms pulse with 10% duty factor.

The modulated signal is frequency translated with the aide of two sources (LO 1 of 2130 to 2310 MHz and LO 2 of 960 MHz), each with an output peak-power level of 13 dBm, and presented to the transmit module. The output of the transmit module is directed to the power amplifier, which has a peak input power level of about 10 dBm (measured as 9.4 dBm). The output of the power amplifier is fed to the spectrum analyzer via an L-band 50-dB directional coupler (with a 50 Ω output termination) at an RF of 1300 MHz and BW of 10 MHz for measurement of the gain and output power. The 50-dB coupled path is fed to a 30-dB attenuator (not shown in Fig. 13) to protect the spectrum analyzer. The spectrum analyzer is set in the time-gated measurement mode and used to make a measurement only when a pulse is present at its trigger input port. The trigger pulse is the same pulse as that used to modulate the 45-MHz CW tone but is delayed and the spectrum analyzer measurement window is adjusted to 25 μ s in order to capture the signal at the appropriate time.

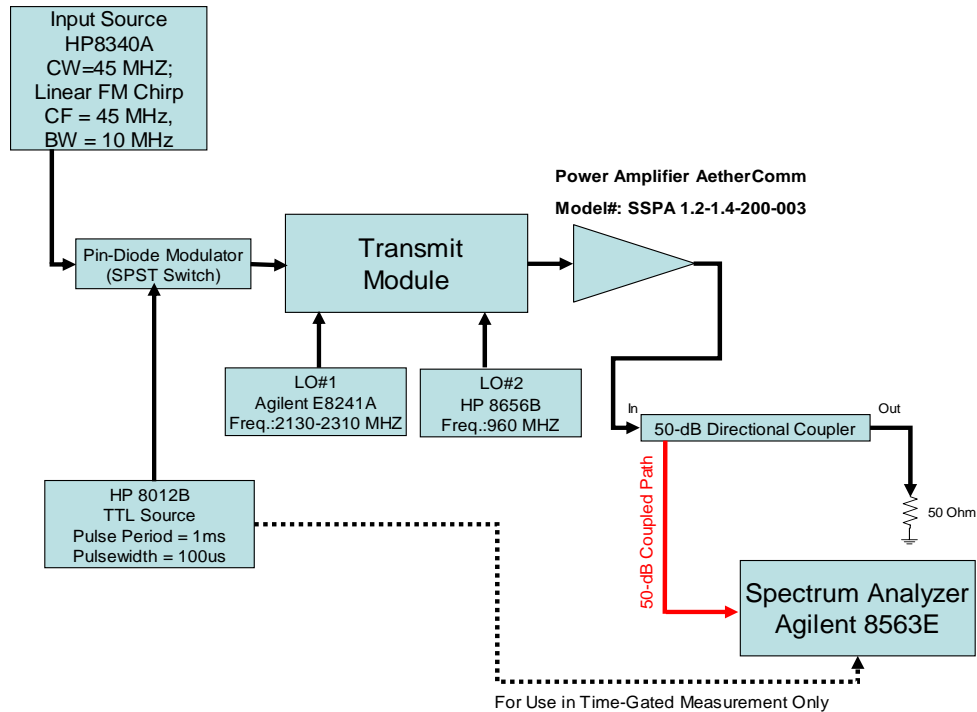


Fig. 13 — Testbed for the characterization of the transmit module

Figure 14 is the output spectrum of the transmit module/power amplifier series combination. This signal was used to determine the gain of the power amplifier and its output power and to examine the output spectrum for any spurious activity in the entire 200-MHz band. The results of the output from the 30-dB attenuator are shown in the figure. The peak power level of the signal is displayed as -29.83 dBm and when the amount of signal attenuation (30 dB from the pad plus 50 dB from the coupled path plus 3.9-dB cable loss for a total of 83.9 dB) is added to this peak level, the peak power at the output of the power amplifier was found to be 53.9 dBm). The gain of the power amplifier is thus 44.5 dB. The highest spurious activity for this amplifier is down 60 dB with respect to the carrier at the CW frequency range of 1215 to 1279 MHz. The worst-case spurs, located at 1216 MHz, are at a ± 71.5 -MHz offset from the carrier.

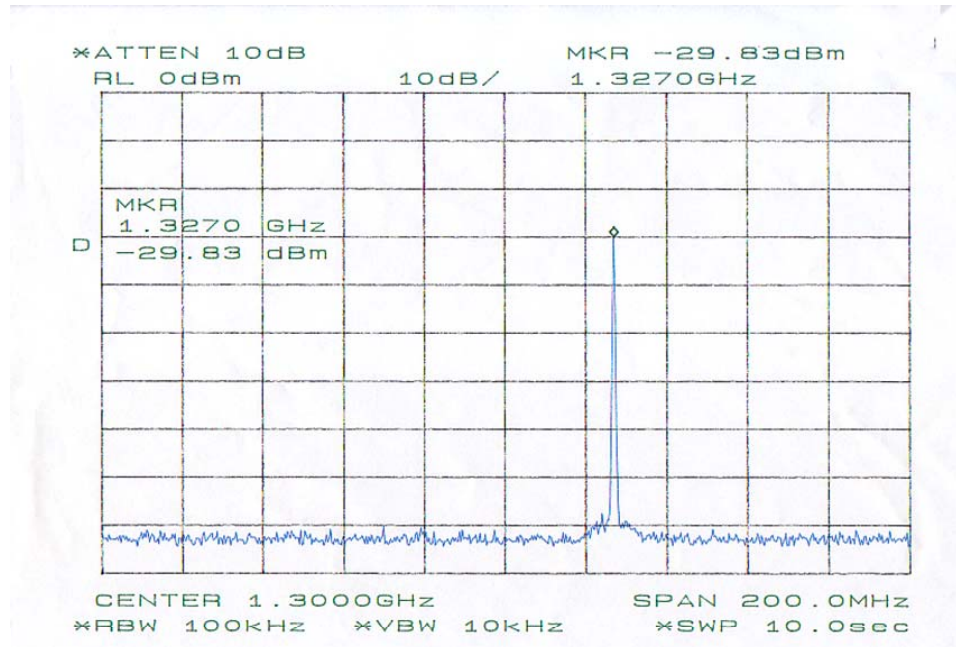


Fig. 14 — Output spectrum of the combined transmit module/power amplifier

Figure 15 is the output spectrum of the transmit module/power amplifier combination using a LFM chirp with 0-dBm peak power as the input signal, which has an F_c of 45 MHz and a BW of 10 MHz. The signal was used to measure how clean the output spectrum was when using the LFM Chirp. The same testbed configuration (with the first LO at 2.23094 GHz and the second LO at 960 MHz) was used for this test. However, no time-gated measurement was needed for this experiment.

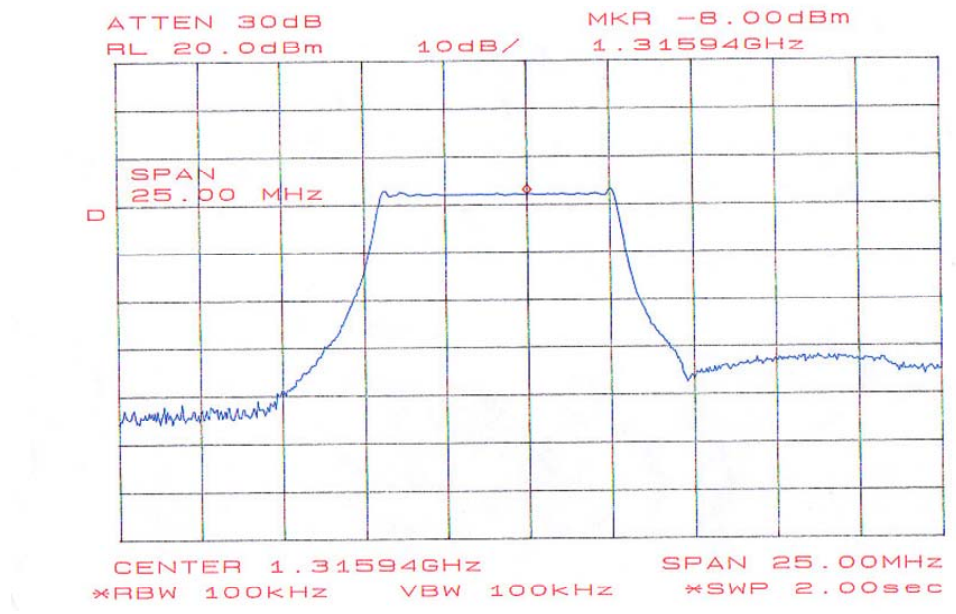


Fig. 15 — Output spectrum of the transmit module/power amplifier combination using an LFM chirp with 0-dBm peak power as the input signal

The calculated and measured transmit module performance characteristics including gain, SFDR, TOI, and total peak power are shown in Table 4. It should be noted that confirmation of the transmit module SFDR and TOI characteristics by measurement is unavailable at the time of this writing since the module is on extended operational assignment for an indeterminable period of time.

Table 4 — Transmit Module Calculated and Measured Parameter Results

Parameter	Calculated	Measured
Gain	10.0 dB	9.4 dB
SFDR	80 dB	N/A
TOI	37.8 dBm	N/A
Total Peak Power	55.0 dBm	53.9 dBm

5.2 Receive Module

As shown in Fig. 4, each receive array antenna element feeds a receive module that in turn feeds a digital baseband converter in the control system section. When the receive array senses the RF energy return scattered from a target, the RF signal from each receive element is downconverted to an IF for digital processing. The downconverted signal is sent to the DSP Section for baseband conversion, data collection, and digital post-processing including VSAR, STAP, and DPCA. The critical receiver parameters are the receiver gain, NF, SFDR, TOI, and P1dB.

Figure 16 is a block diagram of the testbed used to characterize the receive module. Using this configuration, the gain, NF, P1dB, and the SFDR were determined. The input source provides a CW tone centered at 1300 MHz or a frequency-swept chirp signal with an F_c of 1300 MHz and a BW of 10 MHz. This signal at -20 -dBm peak power level is attenuated by 20 dB, using the HP 8495B variable attenuator, to ensure that the receive module operates in the linear region during gain and NF measurement testing. The input peak power level to the module is thus -40 dBm with an F_c of 1300 MHz and BW of 10 MHz, which is frequency translated with the aid of two LO sources (LO 1 of 2215 MHz and LO 2 of 960 MHz), each with a peak output power level of 13 dBm.

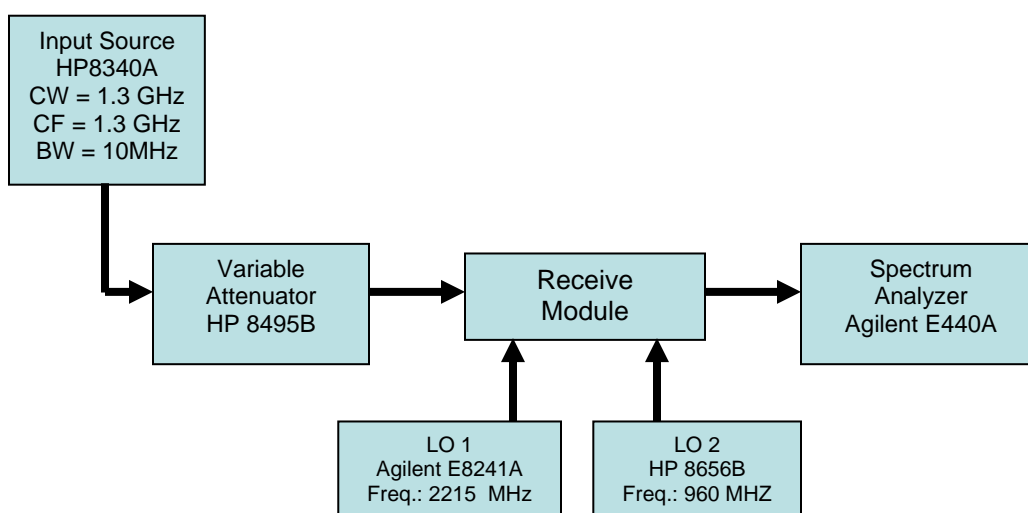


Fig. 16 — Testbed for the characterization of the receive module

The output of the receive module is directed to the spectrum analyzer at an IF of 45 MHz and BW of 10 MHz for measurement of the gain and NF. The parameters P1dB and SFDR are derivable quantities, which are determined from power sweep measurements. In this testing, the peak power level of the 1300-MHz CW tone is used to determine the input power vs output power gain curve. Both the P1dB and SFDR can be determined from this gain curve. The spectrum analyzer plot images as shown in the following figures were used to determine the gain, NF, SFDR, and P1dB.

Figure 17 is the spectrum of the first LO of the TUL UAV radar receiver with an F_c of 2215 MHz and a peak power level of 13 dBm. Figure 18 is the spectrum of the second LO of the radar receiver with an F_c of 960 MHz and a peak power level of 13 dBm.

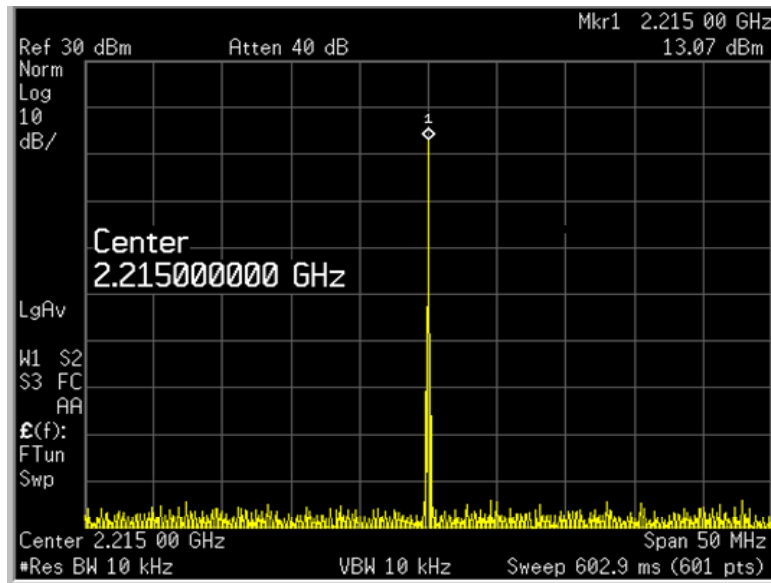


Fig. 17—Spectrum of the radar receiver first LO with 2215-MHz F_c and 13-dBm peak power level

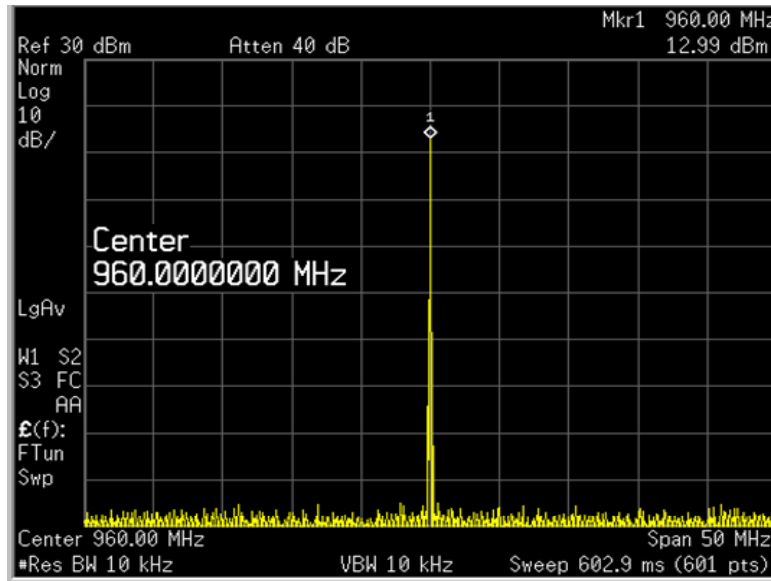


Fig. 18—Spectrum of the radar receiver second LO with 960-MHz F_c and 13-dBm peak power level

Figure 19 is the spectrum of the input signal used to determine the radar receiver gain and NF. The input signal is an LFM chirp with an F_c of 1300 MHz and a BW of 10 MHz. The signal peak power level is -40 dBm and its SNR is 50 dB as approximated by noting the number of divisions between the noise floor and the location of the peak level of the spectrum. It should be noted that the spectrum analyzer does not give true absolute peak values of the spectrum, but instead provides spectral density values (power level in dBm per video BW in Hz) for signals that have finite BW. Thus, the spectrum analyzer power-level reading of -58.61 dBm indicated in Fig. 19 should be understood as -58.61 dBm/1 kHz. It should also be noted that SNR values are given in dB since the noise floor and peak spectral density value of the spectrum have the same dimension.

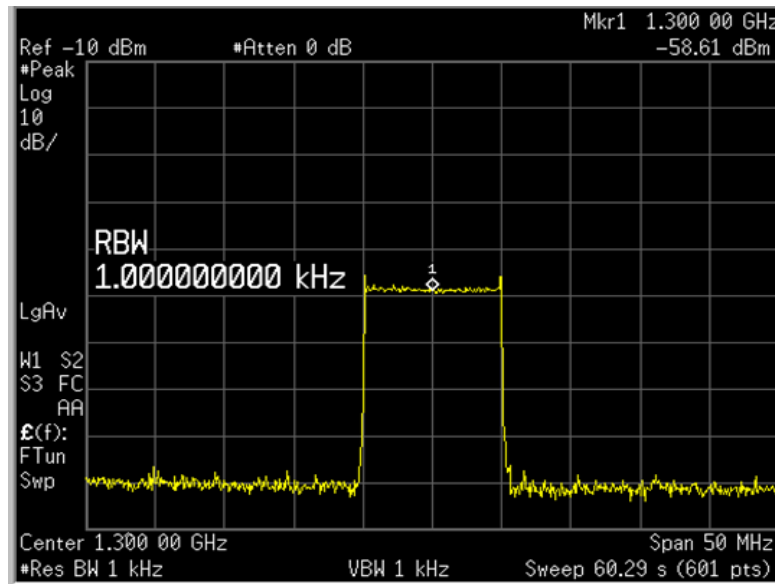


Fig. 19 — Spectrum of input signal used to measure gain and NF of the radar receiver (LFM chirp with 1300-MHz F_c , 10-MHz BW, -40 -dBm peak power, and 50-dB SNR)

Figure 20 is the spectrum of the output signal of the receive module used to determine the gain and NF of the radar receiver. The signal is an LFM chirp with F_c of 45 MHz and BW of 10 MHz. The spectrum analyzer gives a peak-power spectral density reading of -34.93 dBm/1 kHz and the output SNR is approximately 80 dB. The gain of the receive module can be determined by taking the difference between the input and output peak spectral densities at 45 MHz (i.e., $-34.93 - (-58.61)$) and thus the measured gain of the receive module is 23.68 dB. It should be noted that the signal-calibration card was not used in the testbed and is not a factor in the measurement result. The NF was calculated by taking the difference of the input and output SNRs and subtracting out the gain (i.e., $\text{abs}(50 - 80) - 23.68 = 30 - 23.68$) and thus the measured NF is 6.32 dB.

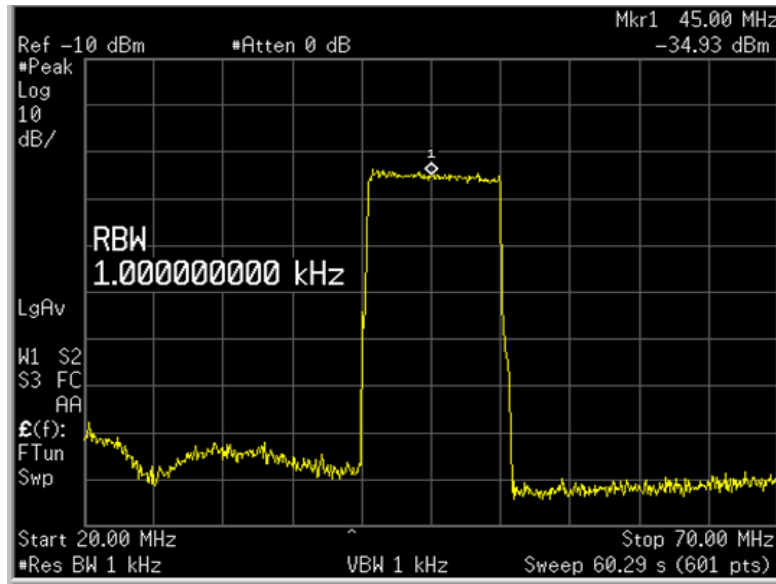


Fig. 20 — Spectrum of receive module output signal used to measure gain and NF of radar receiver (LFM chirp with 45-MHz F_c , 10-MHz BW, and 80-dB SNR)

Figure 21 is a plot of the gain curve of the receive module. It was obtained using the testbed configuration shown above in Fig. 16. The curve can be segmented into two portions. One is the linear portion, which appears to be a straight line, and the nonlinear portion, which is shown as the nearly flat portion of the curve. The linear region has a slope of 1, which refers to the polynomial order of the relationship between input power and output power in the dB scale. As long as the input power level is in this region of values, the device will behave as a predictable linear device (i.e., the output spectrum of the device will not have unwanted spurs and IMD products). Although this device has a rated finite gain of 23.62 dB, it does not have infinite output power.

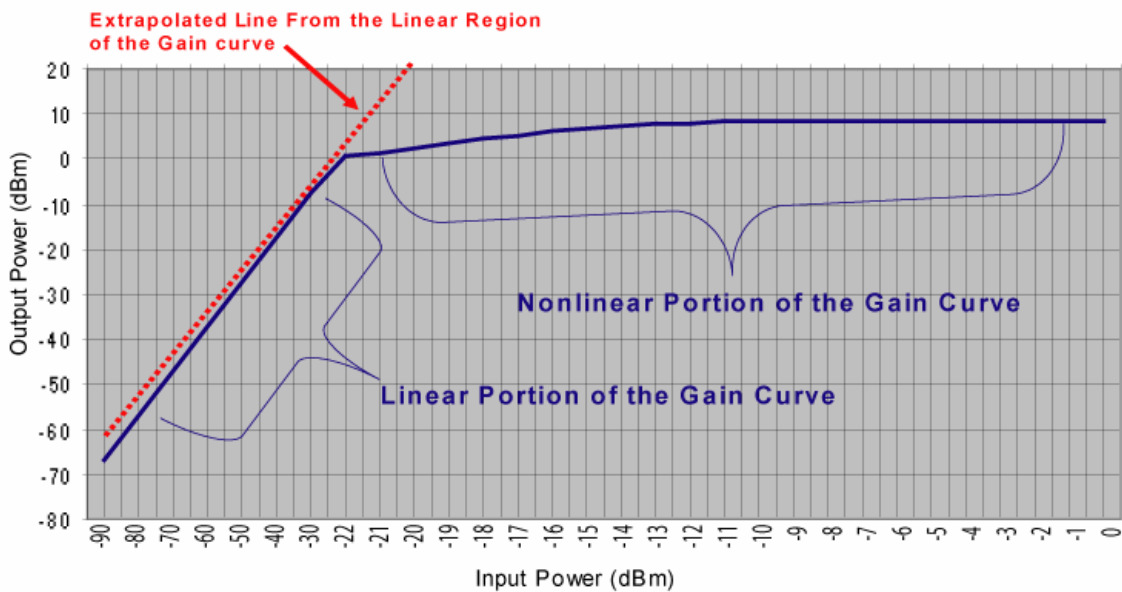


Fig. 21 — Gain curve of the receive module

The nonlinear region of the gain curve shows that there is limit to how much input power the receive module can handle and how much output power it can provide. In this nonlinear region, the output power levels are nearly constant, which is a reflection of the maximum power available from this device.

The transition point, where the linear region meets the nonlinear region, is the point at which the device is in gain compression. This is considered to be the P1dB point and it is used to assess the linearity and maximum output power of the device. This curve is used to determine the P1dB and the SFDR of the receive module. The gain curve is determined by placing a 1300-MHz CW signal at the input of the receive module and adjusting the input peak power level and recording the peak output power level. Using this curve, P1dB can be determined by extrapolating the linear portion of the curve and finding the 1.0-dB deviation between the extrapolated line and the gain curve. The deviation occurs at an input power level of approximately -21.0 dBm, which corresponds to an output power level of 1.53 dBm. This information will be used to measure the SFDR as explained below.

Figure 22 is the spectrum of the input signal used to measure the SFDR. This CW tone is at a power level that places the receive module into gain compression. The SFDR is defined for a specified bandwidth (e.g., 10 MHz centered about the carrier) and is determined by taking the ratio between the peak output power level of the carrier (at 45 MHz in this case) and the frequency spur (nonharmonically related frequency component) with the highest power level.

Figure 23 is the output spectrum of the receive module that is produced by the 1300-MHz input signal. The output signal is attenuated by a 15-dB pad before being fed to the spectrum analyzer. The receive module is in gain compression due to the input signal's -21.26-dBm power level. As shown in Fig. 23, a spur occurred within the 10-MHz region about the 45-MHz carrier. The SFDR, which is the difference between the peak power level of the carrier and the peak power level of the spur, is 78.25 dB (shown in Fig. 23 as -78.25 dB due to a measurement anomaly).

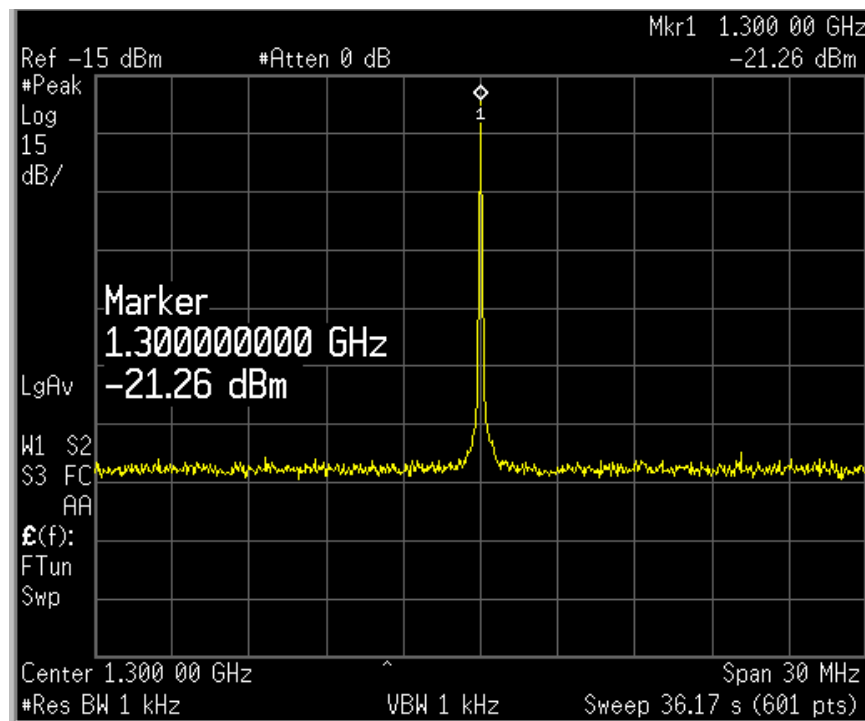


Fig. 22 — Spectrum of the input signal used to measure the SFDR of the receive module

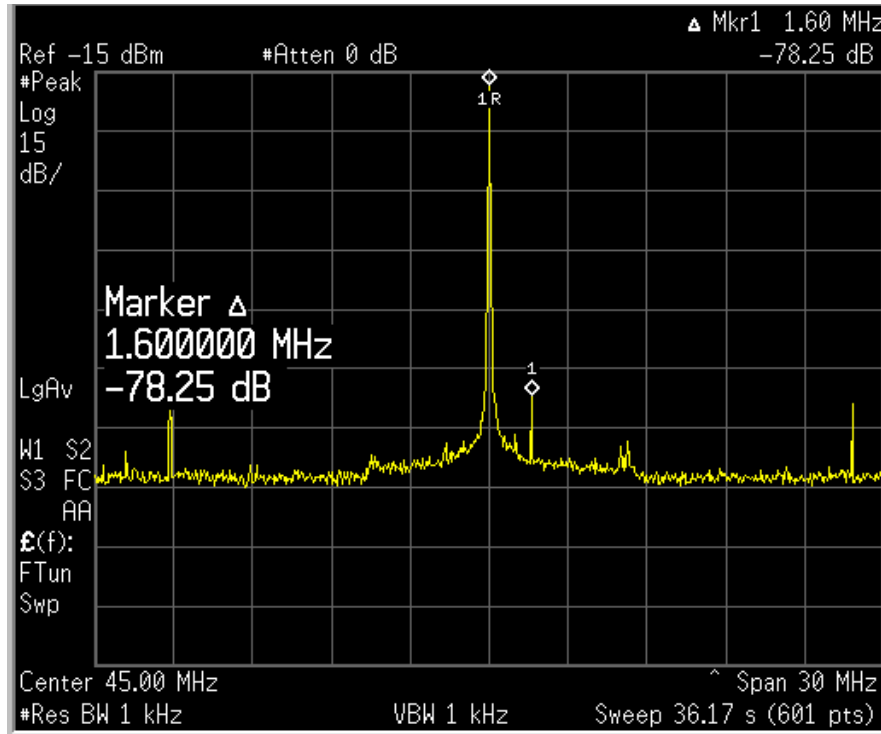


Fig. 23 — Output spectrum of the receive module produced by the 1300-MHz input signal

Figure 24 is the testbed setup for the two-tone test used to determine the second-order IMD ratio needed to calculate the TOI for the receive module. The TOI is a parameter used to measure the linearity of a device when that device is active with an input power level near P1dB. The test consists of injecting two CW signal tones at the input of the receive module by means of two directional couplers. The two CW signals, are set very close together in frequency (100 kHz apart) at 1.3000 GHz and 1.3001 GHz and the power levels of the tones, which must be the same for both, are adjusted to be near the P1dB point (approximately -20 dBm). The two directional couplers are connected in series at the input port of the first coupler (the output port of which is terminated with a 50 Ω load) and the output port of the second coupler in order to provide the best isolation between the two signals. The tones are produced by frequency sources 1 and 2, injected through the directional couplers 1 and 2, respectively, via the 20-dB coupled path and fed to the variable attenuator. The variable attenuator is set to the lowest attenuation level in order to reduce the strength of the two CW signals by 1 dB. The CW tones are then downconverted by the receive module, attenuated by a 20-dB pad (to protect the spectrum analyzer), and fed to the spectrum analyzer for examination. The input and output spectra used in the two-tone test are shown in Figs. 29 and 30, respectively.

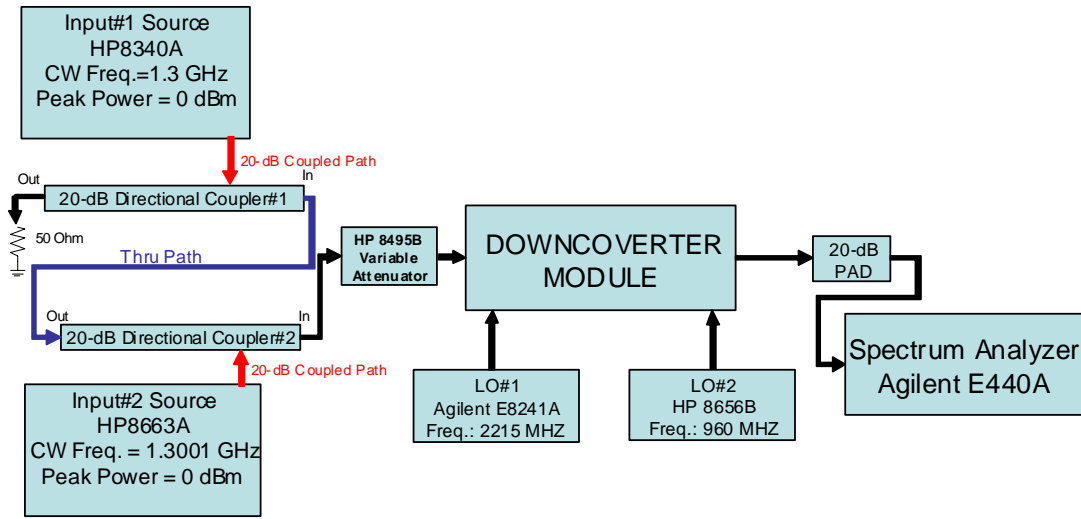


Fig. 24 — Testbed setup for the two-tone test used to determine the second-order IMD ratio for the receive module

Figure 25 is the input spectrum used in the two-tone test for the receive module. The signals were examined by placing the output of the variable attenuator in series with the 20-dB pad at the input to the spectrum analyzer. As seen in Fig. 25, the two tones are at nearly the same power level and are separated in frequency by 100 kHz.

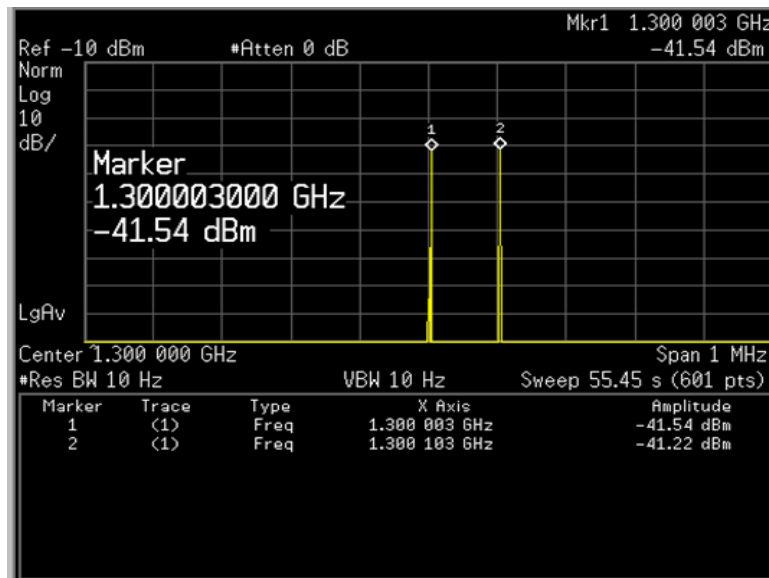


Fig. 25 — Spectrum analyzer image of the input spectrum used in the two-tone test for the receive module

Figure 26 is the spectrum resulting from the two-tone test for the receive module. The signals were examined by placing the output of the receive module in series with the 20-dB pad at the input of the spectrum analyzer as shown above in Fig. 24. The power levels and frequency locations for the two downconverted CW tones (indicated by markers 1 and 2) and the second-order IMD products (indicated by markers 3 and 4) are displayed in Fig. 26. With $F_1 = 1.300$ GHz and $F_2 = 1.3001$ GHz (translated to $f_1 = 45.0$ MHz and $f_2 = 45.1$ MHz, respectively), the second-order IMD products are then located at two frequencies in the spectrum, namely at $2*f_1 - f_2 = 44.9$ MHz and at $2*f_2 - f_1 = 45.2$ MHz. The second-order IMD ratio is determined by taking the difference of the power levels between one of the CW tones (e.g., $f_1 = 45.0$ MHz at a peak power of -18.52 dBm) and one of the second IMD products (e.g., $2*f_1 - f_2 = 44.9$ MHz at a peak power of -96.80 dBm), i.e., $-18.52 - (-96.80) = 78.28$ dB. Therefore, the second-order IMD ratio = 78.28 dB. Finally, the TOI point is calculated from the second IMD ratio by using the relationship, $\text{TOI} = \text{Power Level at } f_1 + \frac{1}{2} * (\text{second IMD Ratio})$. In this case, the $\text{TOI} = -18.52$ dBm + 39.14 dB = 20.62 dBm. This result is based on an actual spectrum observation during testing with the power level of marker 3 exceeding that of marker 4. However, the levels were fluctuating and at the instant that the spectrograph of Fig. 26 was recorded, marker 4 exceeded marker 3. This variation would result in a 1.25 dB reduction in the measured TOI. It should be noted that the signal-calibration card was not used in the testbed and is not a factor in this measurement result.

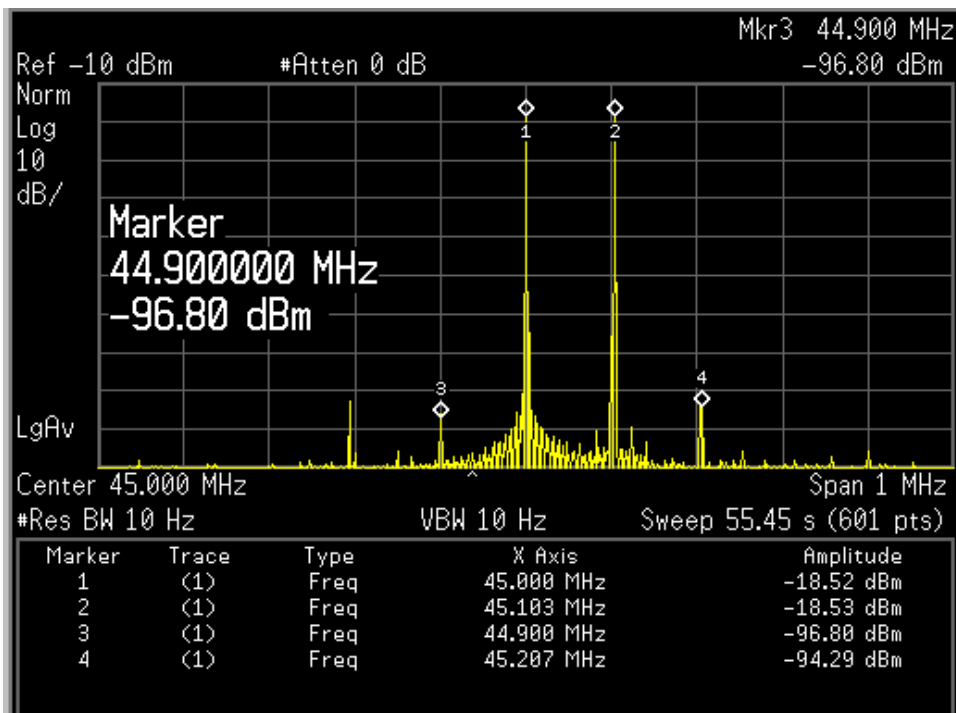


Fig. 26 — The output spectrum used in the two-tone test for the receive module

Table 5 provides the receive module calculated and measurement values for the key parameters including gain, NF, SFDR, TOI, and P1dB. It should be noted that the measured receiver gain was within 1 dB of the calculated value. The NF was calculated to be 5.0 dB but accounting for about 1.3 dB of measured loss due to improper component mounting, the calculated value used in Table 5 was estimated to be 6.3 dB, which compares very well with the measured value. The difference between the calculated and the measured SFDR can be attributable to PCB losses. There was no specification for the receive

module P1dB but the peak power at the output of the receiver had to be less than 4 dBm. However, the receive module P1dB was measured as 1.53 dBm as indicated in Table 5.

Table 5 — Receive Module Calculated and Measured Parameter Results

Parameter	Calculated	Measured
Gain	24.6 dB	23.68 dB
NF	6.3 dB	6.32 dB
SFDR	80 dB	78.25 dB
TOI	21.3 dBm	20.62 dB
P1dB	N/A	1.53 dBm

6. SUMMARY AND CONCLUSIONS

The NRL Radar Division has developed the RF section of a UAV radar system in support of the Navy's TUL UAV Program. This RF section consists of an LO and timing-circuitry module, transmit and receive modules, and a calibration network. The objective of the UAV Radar project was to develop and demonstrate the feasibility of a target detection concept for the TUL UAV system. This concept includes hardware and DSP algorithms for target detection in high clutter and foliage with low false-track rates. A truck-mounted design was chosen and implemented to meet the requirements and simulate a UAV-mounted system, and a prototype was constructed and tested.

Where appropriate, measured transmit and receive module performance parameters were presented here and compared closely with the required calculated parameters. The resulting testbed radar weight and size were within the objective range of less than 300 lb with transmit and receive module PCB area of 4.5 in. × 15 in. and a nominal height of up to 1.0 in. An operational UAV implementation would require a 150 lb maximum radar weight necessitating that the four transmit modules and 24 receive modules each be limited to a weight of less than 8 oz with a PCB area of no more than 4.0 in. by 6.0 in. and height of no more than 1.0 in. This might be achievable with the current testbed components with careful redesign of component layout and close thermal and EMI/RFI management. Furthermore, the latest available low-cost COTS cell-phone components would permit the use of direct upconversion and downconversion processing to reduce the need for some of the current testbed's components, such as mixers and SAW bandpass filters. This would provide for the further reduction of transmit and receive module weight and size as required to achieve an operational UAV radar. The testbed implementation thus shows the promise of lightweight and size-appropriate operational UAV radar implementation at reasonable cost. The effort described in this report represents a significant contribution to the Navy's ability to field an operational TUL UAV in the near future with a radar capability in support of the Fleet.

7. ACKNOWLEDGMENTS

The authors thank Dr. Ben Cantrell, Hugh Faust, Steven Brockett, James Hansen, Kim Scheff, Lawrence Cohen, Dennis Baden, Edward Kutrzyba, Dr. Surendra Samaddar, Jean de Graaf, and Richard Frisby for their assistance during the course of this project.

REFERENCES

1. M. Picciolo, B. Cantrell, E. Kutrzyba, S. Schutz, M. Parent, J. Alatishe, and S. Talapatra, "UAV Radar," *National Military Sensing Symposium (MSS)*, Gettysburg, PA, November 2001.
2. B. Friedlander and B. Porat, "VSAR: A High Resolution Radar System of Ocean Imaging," *IEEE Trans. Aerospace and Electron. Systems* **34**(3), July 1998.
3. M. Richards, "The Concept of Clutter Suppression Interferometry (CSI): Adaptive Displaced Phase Center Antenna (DPCA) Processing + Angle Interferometry," Technical Memorandum, Georgia Tech Research Institute, 13 October 1998.
4. D. Baden, E. Kutrzyba, R. DeOcampo, A. DesRosiers, M. Parent, J. Alatishe, and S. Talapatra, "Multi-Element Foliage Penetration UAV Radar," *2004 Tri-Service Radar Symposium Proceedings*, June 2004.
5. D.M. Pozar, *Microwave Engineering* (J. Wiley and Sons, Inc., New York, NY, 1998), Ch. 3, pp. 175-176.

ABBREVIATIONS AND ACRONYMS

ADC	analog-to-digital converter	P1dB	P1dB compression point
COTS	commercial-off-the-shelf	PCB	printed circuit board
DAC	digital-to-analog converter	PLL	phase-locked loop
DPCA	displaced phase center antenna	PW	pulsewidth
DSP	digital signal processing	PRF	pulse repetition frequency
EM	electromagnetic	PRI	pulse repetition interval
F_c	center frequency	RF	radio frequency
FIR	finite impulse response	SAR	synthetic aperture radar
FO	fiber optic	SAW	surface acoustic wave
FPGA	field programmable gate array	SFDR	spur-free dynamic range
GMTI	ground moving target indicator	SNR	signal-to-noise ratio
GUI	graphical user interface	SPST	single-pole single-throw
IF	intermediate frequency	STAP	Space Time Adaptive Processing
IMD	intermodulation distortion	TEM	transverse electromagnetic
LO	local oscillator	TOI	third-order intercept
LNA	low-noise amplifier	TUL UAV	Tactical Ultra-Light UAV
LPF	low-pass filter	TTL	transistor-to-transistor logic
MMIC	monolithic microwave integrated circuit	UAV	Unmanned Aerial Vehicle
NF	noise figure	VME	Virtual Machine Environment
NRL	Naval Research Laboratory	VSAR	Velocity SAR
		VTUAV	Vertical Tactical UAV